

ASTROPHYSICALLY RELEVANT NEUTRON CAPTURE NEAR THE BORDER OF STABILITY

P. Mohr and H. Oberhummer

*Institut für Kernphysik, Technische Universität Wien,
Wiedner Hauptstraße 8–10, A–1040 Vienna, Austria*

H. Beer

*Forschungszentrum Karlsruhe, Institut für Kernphysik III,
P.O. Box 3640, D–76021 Karlsruhe, Germany*

The neutron capture cross section on ^{26}Mg was measured in the astrophysically relevant energy region from 25 keV to 220 keV. The experimental results agree well with a calculation using the Direct Capture (DC) model together with systematic folding potentials. This experiment confirms for the $^{26}\text{Mg}(n,\gamma)^{27}\text{Mg}$ reaction that the DC process is at least comparable to the Compound-Nucleus (CN) process. The reliability of DC calculations is discussed, and we present some ideas for future experiments which could reduce the theoretical uncertainties of DC calculations.

1 Introduction

Low-energy neutron capture is very important for the nucleosynthesis in stars. Capture cross sections on neutron-rich stable nuclei close to the border of stability at thermonuclear energies ($kT \approx 8 - 100$ keV) are required for s -process calculations. For the α -rich freeze-out in Type II supernovae and for the r -process one needs capture cross sections on stable and unstable neutron-rich nuclei at somewhat higher energies ($kT \approx 50 - 250$ keV). The cross sections for the s -process can be measured, but neutron capture experiments on unstable nuclei are in general not possible.

Up to now calculations of r -process capture cross sections on unstable nuclei have mainly been performed using the statistical Hauser-Feshbach (HF) model where the capture cross section is derived from penetration probabilities and the level density in the compound nucleus (CN); even though the importance of the Direct Capture (DC) process was recognized in the last years it was not used in r -process calculations. (See, e.g.¹: “Of course, in these cases, the validity of the adopted Hauser-Feshbach rate predictions has to be questioned, the neutron capture process being possibly dominated by direct electromagnetic transitions to a bound final state rather than through a compound nucleus intermediary. . . This complication is neglected here.”)

A high level density in the CN is necessary for the application of the HF model. Almost all intermediate and heavy stable nuclei fulfill this condition,

because the neutron binding energy is of the order of about 7–10 MeV. However, for neutron-rich nuclei involved in the r -process the binding energies decrease down to zero at the neutron dripline, and therefore the level density in the CN becomes very small. This behavior is shown schematically in Fig. 1. The DC process can be analyzed experimentally for neutron-rich light and some intermediate nuclei (especially with magic neutron number) where the binding energies are of the order of 4–6 MeV. A series of experiments was performed at the Karlsruhe Van de Graaff accelerator (FZK): $^{15}\text{N}^2$, $^{18}\text{O}^3$, $^{36}\text{S}^4$, $^{48}\text{Ca}^5$.

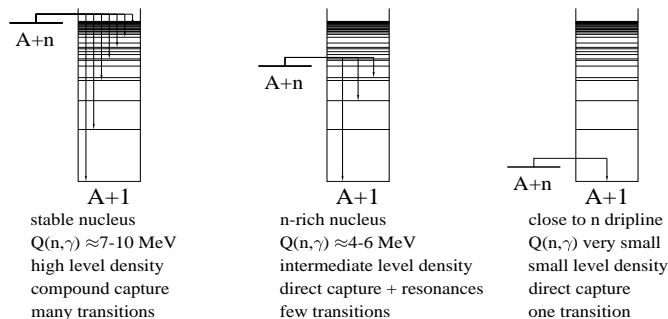


Figure 1: Schematic presentation of energy levels relevant for (n,γ) capture reactions on nuclei with high, intermediate, and low neutron separation energy (from left to right).

These measurements have to be supplemented by DC calculations of (n,γ) capture cross sections on more neutron-rich unstable target nuclei in the isotopic chain. Experimental information to improve these calculations can be obtained from (d,p) reactions using accelerated neutron-rich fission fragments and inverse kinematics.

2 Present Experiments

For the measurement of small capture cross sections often the activation method is used. This method is only applicable for unstable residual nuclei with halfives longer than about 1 h. For nuclei with shorter halfives the fast cyclic activation method was developed at the Van-de-Graaff laboratory of the Forschungszentrum Karlsruhe⁶: The sample is irradiated for a short time (comparable or shorter than the halfife), then the sample is moved from the irradiation position to the counting position, and the γ -rays following the β -decay of the residual nuclei are detected using a high-purity germanium (HPGe) detector. To gain statistics, this procedure can be repeated many times.

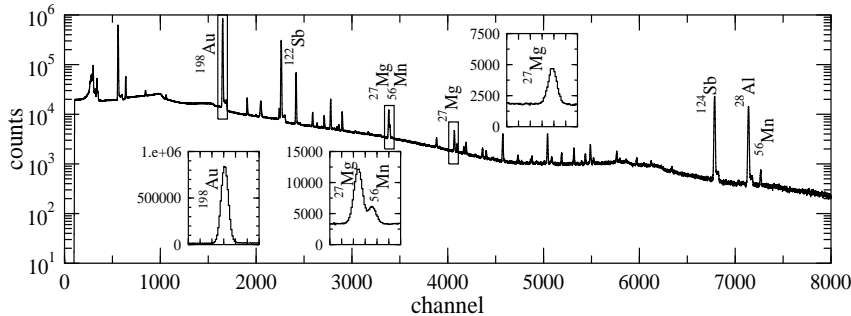


Figure 2: Typical γ -ray spectrum from the activation measurement of $^{26}\text{Mg}(n,\gamma)^{27}\text{Mg}$. The insets show the three regions of interest (^{198}Au , $E_\gamma = 412$ keV; ^{27}Mg , $E_\gamma = 844, 1014$ keV).

The neutrons for the activation experiment are generated by the $^7\text{Li}(p,n)^7\text{Be}$ reaction using beam currents of about $100 \mu\text{A}$. At a proton energy close above the reaction threshold ($E_p^{\text{thres}} = 1881$ keV) a quasi-thermal spectrum with $kT \approx 25$ keV is obtained. At somewhat higher energies neutron spectra with a width of about 20–30 keV were generated.

For the ^{26}Mg experiment the sample consisted of a small tablet of 98.79% enriched ^{26}MgO (diameter 6 mm, weight 90 mg) which was sandwiched between two thin gold foils to determine the $^{26}\text{Mg}(n,\gamma)^{27}\text{Mg}$ relative to the well-known $^{197}\text{Au}(n,\gamma)^{198}\text{Au}$ cross section. The residual nucleus ^{27}Mg decays with a half-life of 9.458 ± 0.012 min to ^{27}Al which deexcites by γ -ray emission with $E_\gamma = 844$ keV (branching $71.8 \pm 0.4\%$) and $E_\gamma = 1014$ keV ($28.0 \pm 0.4\%$)⁷. A typical spectrum is shown in Fig. 2, and the experimental cross section is compared to a DC calculation in Fig. 3.

3 Theoretical Analysis

The capture cross section was calculated using the DC model^{8,9}:

$$\sigma_{DC} \sim \sum_i C^2 S_i \cdot | \langle u_{NL,i}(r) | \mathcal{O}^{E\mathcal{L}/M\mathcal{L}} | \chi_L(r) \rangle |^2 \quad (1)$$

with $C^2 S_i$: spectroscopic factors of the final states, $u_{NL,i}(r)$: bound state wave functions, $\chi_L(r)$: scattering wave function, and $\mathcal{O}^{E\mathcal{L}/M\mathcal{L}}$: transition operators of electromagnetic $E\mathcal{L}$ and $M\mathcal{L}$ transitions.

For the calculation of the wave functions we used systematic folding potentials

$$V_F(r) = \lambda \cdot \int \int \rho_P(r_P) \rho_T(r_T) v_{eff}(s, \rho, E) d^3 r_P d^3 r_T \quad (2)$$

with ρ_P and ρ_T being the densities of projectile and target, and an effective nucleon-nucleon interaction v_{eff} ^{10,11,12}. Compared to standard Woods-Saxon potentials the number of parameters is reduced because the shape of the potential is determined by the folding procedure.

The potential strength parameter λ is adjusted to the binding energy (bound states) and to the scattering length (scattering wave function) leading to λ values close to unity. The p -wave potential has to be reduced by about 15% in strength to obtain a good description of the measured $^{26}\text{Mg}(n,\gamma)^{27}\text{Mg}$ data. The spectroscopic factors were taken from a $^{26}\text{Mg}(d,p)^{27}\text{Mg}$ experiment¹³.

The results of the DC calculations for all strong transitions of the capture reaction $^{26}\text{Mg}(n,\gamma)^{27}\text{Mg}$ are shown in Fig. 3, and the astrophysically relevant reaction rate per particle pair $N_A \langle \sigma \cdot v \rangle$ is shown in Fig. 4.

E_x (keV)	J^π	C^2S_{exp}	C^2S_{th}	$C^2S_{(n,\gamma)}$
0	1/2 ⁺	0.57 – 1.07	0.43 – 0.70	–
984.7	3/2 ⁺	0.37 – 0.80	0.28 – 0.45	–
1698.0	5/2 ⁺	0.13 – 0.31	0.02 – 0.14	–
3559.5	3/2 ⁻	0.40 – 0.56	–	0.37
3760.4	7/2 ⁻	0.55 – 0.80	–	–
4149.8	(5/2 ⁺)	0.03*	0.001 – 0.06	–
4827.3	(1/2 ⁻)	0.32*	–	0.19*

* assuming (J^π) as given in column 2

Table 1: Spectroscopic factors of $^{27}\text{Mg} = ^{26}\text{Mg} \otimes n$ taken from different experiments^{13,14,15,16} and from shell-model calculations^{13,17,18}. Note that the spectroscopic factors of the states at $E_x = 4149.8$ keV and 4827.3 keV were determined only in one experiment.

For stable nuclei the main uncertainties are given by the spectroscopic factors. An overview of spectroscopic factors obtained from different transfer reactions^{13,14,15,16} and from shell-model calculations^{13,17,18} is given in Tab. 1. Additionally, spectroscopic factors can be derived very accurately⁵ from the thermal capture cross section by the ratio of experimental to calculated cross section (see Tab. 1, last column).

The uncertainties in the potential are relatively small because the s -wave potential which is the only relevant partial wave at thermal energies can be properly adjusted, and the p -wave potential should not differ by more than about 20% from the s -wave potential.

For unstable nuclei far from stability the main uncertainties are obviously given by the unknown spins, parities J^π and excitation energies E_x of the relevant final states in the residual nuclei, because E1 transition probabilities

are proportional to E^3 and E2 transition probabilities even scale with E^5 . Of course, the spectroscopic factors are also uncertain by at least a factor of two for these nuclei but these uncertainties are relatively small compared to the E^3 and E^5 energy dependence of the transitions.

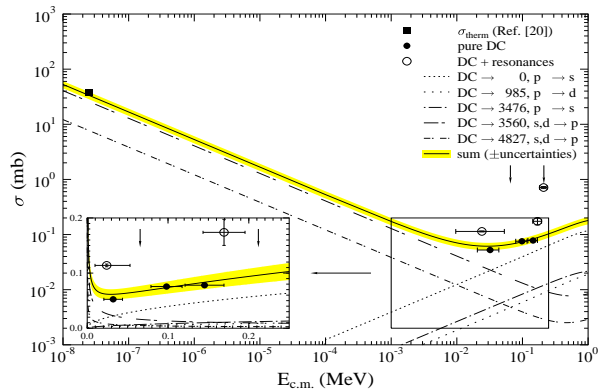


Figure 3: Preliminary cross section of $^{26}\text{Mg}(n,\gamma)^{27}\text{Mg}$. The arrows mark known resonances¹⁹, and the experimental data points shown with open circles are affected by these resonances. (Note that the horizontal error bars show only the FWHM of the neutron energy!) Additionally, the thermal capture cross section²⁰ (full square) is well reproduced.

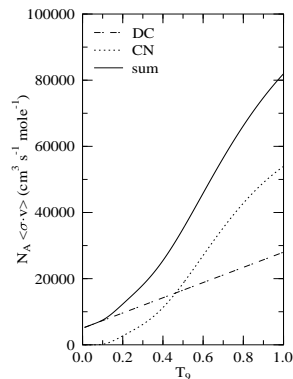


Figure 4: Reaction rate factor $N_A \langle \sigma \cdot v \rangle$ of the neutron capture reaction $^{26}\text{Mg}(n,\gamma)^{27}\text{Mg}$.

4 Future Experiments

Using accelerated neutron-rich fission fragments the input parameters of DC calculations could be determined experimentally by (d,p) reactions at energies in the order of 5–10 MeV/u. The relevant quantities which are spins and parities, excitation energies, and spectroscopic factors can be derived from well-established DWBA analyses of the angular distributions.

Because of the inverse kinematics a relatively low background can be expected in the proton spectra at laboratory backward angles which correspond to forward angles in the center-of-mass system. The deuteron elastic scattering can be measured at the same experiment by detecting the recoil deuterons at laboratory forward angles to derive the deuteron-optical potential. The proton-optical potential for the exit channel can be taken from potential systematics. A sufficient count rate is expected if beam currents in the order of ppA to pnA are obtained, of course, depending on the size of the (d,p) cross section (about 1–100 μb).

5 Conclusions

We measured the DC contribution of the reaction $^{26}\text{Mg}(n,\gamma)^{27}\text{Mg}$ using the fast cyclic activation technique. The experimental results agree reasonably well with our DC calculation. The importance of the DC mechanism even for stable neutron-rich nuclei is again confirmed.

DC calculations of (n,γ) reactions on unstable nuclei depend sensitively on the input parameters, i.e., Q-value of the (n,γ) -reaction, and J^π , E_x , and C^2S of the final states in the residual nuclei. These parameters can be determined experimentally from (d,p) transfer reactions using accelerated neutron-rich fission fragments in reverse kinematics.

Acknowledgments

We would like to thank the technicians G. Rupp, E. Roller, E.-P. Knaetsch, and W. Seith from the Van-de-Graaff laboratory at the Forschungszentrum Karlsruhe. This work is supported by Deutsche Forschungsgemeinschaft (DFG Mo739) and Fonds zur Förderung der wissenschaftlichen Forschung (FWF S7307-AST).

References

1. S. Goriely and M. Arnould, *Astron. Astrophys.* **312**, 327 (1996).
2. J. Meissner *et al.*, *Phys. Rev. C* **53**, 977 (1995).
3. J. Meissner *et al.*, *Phys. Rev. C* **53**, 459 (1995).
4. H. Beer *et al.*, *Phys. Rev. C* **52**, 3442 (1995).
5. H. Beer *et al.*, *Phys. Rev. C* **54**, 2014 (1996).
6. H. Beer *et al.*, *Nucl. Inst. Meth. A* **337**, 492 (1994).
7. P. M. Endt, *Nucl. Phys.* **A521**, 1 (1990).
8. B. T. Kim, T. Izumoto, and K. Nagatani, *Phys. Rev. C* **23**, 33 (1981).
9. K. H. Kim, M. H. Park, and B. T. Kim, *Phys. Rev. C* **35**, 363 (1987).
10. H. de Vries, C. W. de Jager, and C. de Vries, *At. Data Nucl. Data Tables* **36**, 495 (1987).
11. A. M. Kobos *et al.*, *Nucl. Phys.* **A425**, 205 (1984).
12. H. Abele and G. Staudt, *Phys. Rev. C* **47**, 742 (1993).
13. F. Meurders *et al.*, *Nucl. Phys.* **A230**, 317 (1974).
14. I. Turkiewicz *et al.*, *Nucl. Phys.* **A486**, 152 (1988).
15. I. Paschopoulos *et al.*, *Nucl. Phys.* **A252**, 173 (1975).
16. S. Sinclair *et al.*, *Nucl. Phys.* **A261**, 511 (1976).
17. Z. Moroz, *J. Phys. Soc. Jpn. Suppl.* **55**, 221 (1986).

18. R. Bengtsson *et al.*, Phys. Scripta **29**, 402 (1984).
19. H. Weigmann, R. L. Macklin, and J. A. Harvey, Phys. Rev. C **14**, 1328 (1976).
20. S. F. Mughabghab, M. Divadeenam, and N. E. Holden, *Neutron Cross Sections*, Academic Press, New York, 1981.